Fine-Structure Predissociation of Ultracold Photoassociated $^{39}K_2$ Molecules Observed by Fragmentation Spectroscopy

H. Wang, P. L. Gould, and W. C. Stwalley

Department of Physics, U-46, University of Connecticut, Storrs, Connecticut 06269
(Received 13 June 1997)

We report the first observation of fragmentation spectra of the fine-structure predissociated long-range 1_g and 0_u^+ ($b\,^3\Pi_{0^+u}$) states of ultracold ($T < 1$ mK) $^{39}K_2$ molecules. The 1_g state predissociates via the curve crossing at long range ($R \sim 23$ Å) with the repulsive 0_g^+ state. The 0_u^+ state, however, predissociates predominantly through molecular fine-structure mixing at short range with the $b\,^3\Pi_{1u}$ component. Our technique of fragmentation spectroscopy is a sensitive and selective tool for ultracold photoassociation and fine-structure-changing collisions.   [S0031-9007(97)05004-7]

PACS numbers: 32.80.Pj, 33.80.Gj, 34.20.Cf

One of the most interesting applications of laser-ultracold atom interactions is the newly developed photoassociative spectroscopy of ultracold atoms [1,2]. This spectroscopic technique has been very successfully used for precision measurements of long-range interatomic potentials [3,4], molecular dissociation energies [5], atomic radiative lifetimes [3,6,7], and ground-state scattering lengths [8–11]. Photoassociation spectra have previously been generated using two detection techniques: trap loss detection [Li, Na, Rb (see [2] for a review), and K [4]] and two-photon or two-color ionization of the excited molecular states (Na [2,12], K [13], and Rb [14]). The former is very convenient for probing most of the long-range states except for the low vibrational levels of the two "pure long-range" 0_g^- and 1_u states [15] due to the rather small associated local kinetic energies for these levels. Instead, ion detection is particularly effective for detecting the "pure long-range" states as in the experiments with Na [3] and K [4] for the 0_g^- state and very recently with K for the 1_u state [16].

Here we employ a third sensitive and selective technique for detecting photoassociative spectra: fragmentation spectroscopy of predissociating long-range molecular states. Using this technique, we observe for the first time the predissociation of the long-range 1_g state. Although line broadening of the 0_u^+ state (presumably due to predissociation) has been reported in Rb_2 [17], we present the first demonstration of predissociation of the 0_u^+ state by detecting atomic fragments. Since the fine-structure (FS) predissociation described here and the hyperfine-structure (HFS) predissociation recently reported in [18] both involve highly excited vibrational levels near the atomic limit, they provide the near-threshold, channel-selected, experimental tests to the theories of the FS and HFS changing collisions which are very important in the ultracold regime [19–21].

The experimental setup has been previously described in detail [4]. Briefly, a high density vapor cell magneto-optical trap confines a sample of $\sim 10^7$ ^{39}K atoms with density $> 10^{11}$ atoms/cm^3 and a temperature ~ 500 μK.

The trapping and repumping laser beams are provided by a single mode tunable ring Ti:sapphire laser at 766.5 nm. The photoassociation is induced by a second tunable Ti:sapphire laser with output power up to ~ 1 W. Figure 1 shows the excitation scheme of the experiment. First, the colliding ground-state atomic pairs (0_u^-, 1_u, and 0_g^+) are excited to the long-range bound levels of the 1_g or the 0_u^+ states, both dissociating to the higher asymptote $4\,^2S_{1/2} + 4\,^2P_{3/2}$. If these vibrational levels predissociate into the lower fine-structure asymptote, the $4\,^2P_{1/2}$ atomic fragments are excited to the $5\,^2D_{3/2}$ state by a yellow photon $h\nu_2$ (provided by a ring dye laser operated with R-6G dye). The $5\,^2D_{3/2}$ atoms are further photoionized by $h\nu_1$ or $h\nu_2$ with atomic ions (K^+) being collected by a channeltron multiplier. Trap fluorescence is simultaneously monitored by a PMT-filter system.

Figures 2(a), 2(b), and 2(c) show the fragmentation spectra spanning a region of ~ 34 cm^{-1} below the
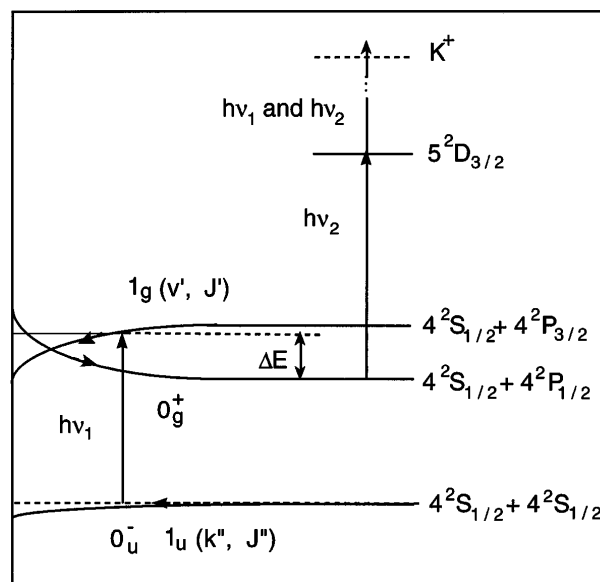
FIG. 1. Excitation scheme of the fragmentation spectroscopy of ultracold photoassociated molecules.
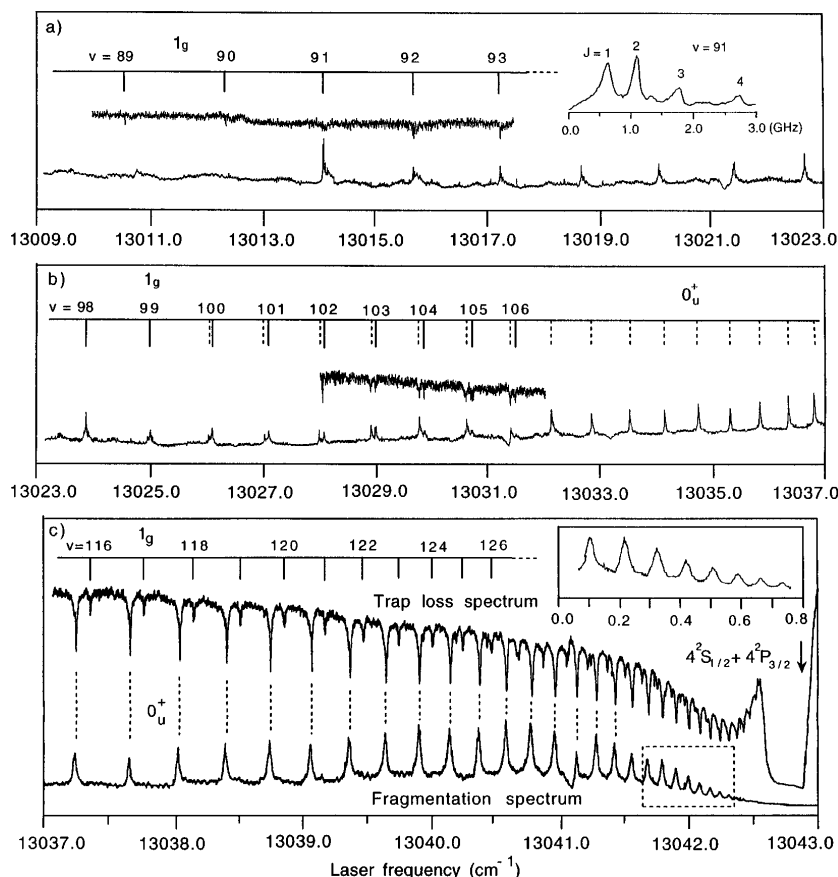
FIG. 2. Fragmentation (lower) and trap loss (upper) spectra of the predissociated long-range 1_g and 0_u^+ states of $^{39}K_2$. (a) The onset of the fragmentation spectrum of the 1_g state at $v = 91$. Lower vibrational levels are still present in the trap loss spectrum. The expanded inset shows the rotational structure of $v = 91$. (b) The 1_g progression is gradually replaced by the 0_u^+ progression. The trap loss spectrum shows both states for comparison. (c) Near the dissociation limit, the 0_u^+ series is the only electronic state observed in the fragmentation spectrum while other series appear in the trap loss spectrum. The inset details the line broadening of the eight vibrational levels in the dashed rectangle.

$4^2S_{1/2} + 4^2P_{3/2}$ limit ($\Delta E_{FS} = 57.71$ cm^{-1}) obtained by recording ions while scanning the photoassociation laser frequency. Given the excitation scheme shown in Fig. 1, it is unambiguous that each resonance in the fragmentation spectra corresponds to a molecular rovibrational state which predissociates. If the photoassociation laser beam is turned off, ion counts due to the weak trapping beams (tuned 40 MHz below the $4^2P_{3/2}$ level) are found to be negligible. We note that the photoassociation laser induces a background in the fragmentation spectrum near the atomic limit shown in Fig. 2(c). This may result from increased off-resonant absorption, followed by FS predissociation, due to the increase in density of states near the asymptote. Similar phenomena have been studied by other authors within a few GHz below the atomic transition [22]. We assign the fragmentation spectra as labeled in Figs. 2(a), 2(b), and 2(c) according to the assignments of our previous trap loss spectra [4]. A striking feature is that the 1_g fragmentation spectrum has an onset in intensity at the level of $v = 91$ [23] while the trap loss spectrum shows lower vibrational levels and no sudden intensity change. Well resolved rotational structures are also recorded, e.g., $v = 91$ in the inset of Fig. 2(a). In Fig. 2(b), between 20 and 10 cm^{-1} below the atomic limit, the 1_g progression becomes weaker while the 0_u^+ vibrational series becomes more pronounced. This 0_u^+ progression is the only electronic state observed near the dissociation limit in the fragmentation spectrum although

three vibrational series, 0_u^+, 1_g, and 0_g^- are observed in the trap loss spectrum (for the weak 0_g^- state, see Ref. [4] for details). Very near the atomic limit, the trap is strongly perturbed by the intense photoassociation laser, resulting in an almost total loss of trapped atoms.

Significant state mixing usually occurs near a curve crossing point. Figure 3(a) shows the five relevant long-range potential curves of $^{39}K_2$ given in [4]. At $R \sim 23$ Å, the attractive long-range 1_g potential (dissociating to the $4^2P_{3/2}$ limit) crosses the repulsive 0_g^+ state potential which dissociates to the $4^2P_{1/2}$ limit. The 1_g state interacts with the 0_g^+ state through the two nontrivial electronic coupling matrix elements $H^{el} = \langle {}^1\Pi_{1g}|\frac{1}{2\mu R^2}\hat{J}^- L^+|{}^1\Sigma_{0g}^+\rangle$ and $\langle {}^3\Pi_{1g}|\frac{1}{2\mu R^2}\hat{J}^-\hat{S}^+|{}^3\Pi_{0g}\rangle$ [4,24]. Here $\hat{J}^\pm = \hat{J}_x \pm i\hat{J}_y$, $\hat{L}^\pm = \hat{L}_x \pm i\hat{L}_y$, and $\hat{S}^\pm = \hat{S}_x \pm i\hat{S}_y$. The nonadiabatic transition probability is equal to the square of the total interaction matrix element $\langle \chi_{v,J}|H^{el}|\chi_{E,J}\rangle$, where $\chi_{v,J}$ and $\chi_{E,J}$ are the bound and free vibrational wave functions. In Fig. 3(a), we plot the observed energy levels and the radial wave functions of the bound 1_g states $v = 85, 91$, and 105 (solid line), and the wave functions of the free 0_g^+ state (dashed line) at the corresponding energies. For $v = 91$, the two major portions of the 1_g and 0_g^+ state wave functions (near their classical turning points) overlap well in phase, resulting in a larger vibrational overlap integral. For levels $v > 91$, these two slowly changing amplitudes become out of phase as shown for $v = 105$, and the overlap
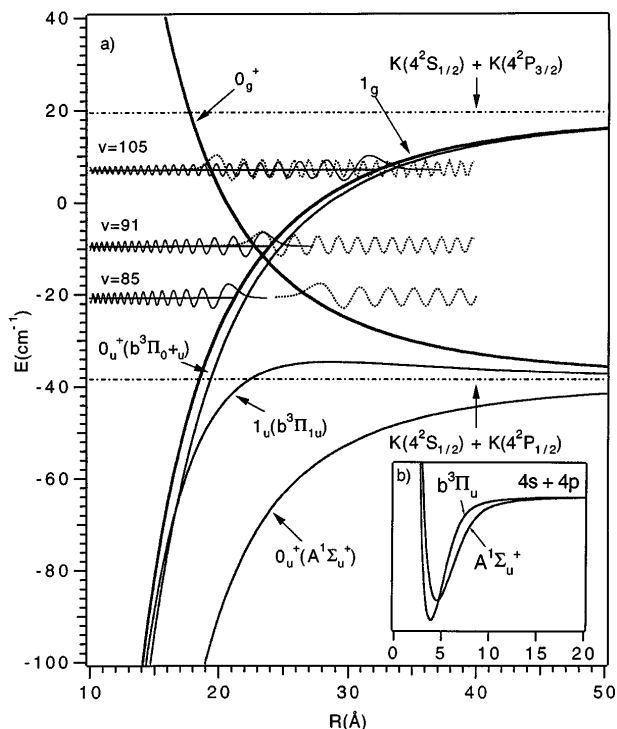
FIG. 3. (a) The five relevant long-range potential curves. The two thicker solid lines are the 1_g and 0_g^+ potentials with a crossing point at $R \sim 23$ Å. The potential curves of the 0_u^+ and the 1_u states (thinner solid) cross at $R \sim 17$ Å. The wave functions (solid = bound, dotted = free) are not normalized. The zero of the vertical axis is the FS degeneracy-weighted center of the $4p$ state. (b) The potential curves of the $b\,^3\Pi_u$ and $A\,^1\Sigma_u^+$ states (7585 and 6328 cm^{-1} in well depth, respectively).

integral (mainly from contributions of the fast-changing amplitude) gradually vanishes as the turning points of the two curves become further separated. For levels $v < 91$, the two wave functions start to become totally separated as for $v = 85$, and the overlap vanishes very quickly due to the rapid decay of the amplitudes around the classical turning points. Given the observed fragmentation spectrum in Fig. 2(a), the level $v = 90$, located 1.67 cm^{-1} below the level $v = 91$ and in the vicinity of the crossing point within the uncertainty of the potential curves (no more than a few tenths of a cm^{-1} in this region), should have a nonadiabatic transition probability at least a factor of 10 smaller than that for $v = 91$. This intensity distribution can be used to determine the electronic coupling matrix element $H^{\rm el}$ and to refine the potential curves as well. The 1_g fragmentation spectrum therefore confirms that the long-range curve crossing at $R \sim 23$ Å is the unique physical origin for the predissociation of the 1_g state and should have a negligible contribution to FS-changing collisions at the asymptotic limit. The predissociation rate of the 1_g state is believed to be smaller than its radiative decay rate (asymptotically $A_{1g} \approx 1.2 A_{4p} = 4.5 \times 10^7$ s^{-1} [7,20]). This is suggested by two facts: (1) The trap loss spectrum shows no sudden change in intensity around $v = 91$, indicating

that predissociation is a small fraction of the total trap loss; and (2) no apparent line broadening is observed. The well resolved rotational lines of $v = 91$ have a linewidth of 140(20) MHz (the uncertainty is 1σ of twelve measurements) due to power broadening.

Three electronic interactions [(I)–(III)] are potentially responsible for the predissociation of the 0_u^+ ($b\,^3\Pi_{0^+u}$) state: (I) the molecular fine-structure mixing with the $b\,^3\Pi_{1u}$ state at short range; (II) the curve crossing with the 1_u state (again the $b\,^3\Pi_{1u}$ component) at long range ($R \sim 17$ Å); and (III) the curve crossing with the $A\,^1\Sigma_u^+$ state at short range ($R \sim 4.7$ Å). The 0_u^+ ($b\,^3\Pi_{0^+u}$) state dissociates to the $4\,^2P_{3/2}$ limit and all three other states to the $4\,^2P_{1/2}$ asymptote. The physics of interaction (I) is that at short range the six components $^3\Pi_{0^\pm u}$, $^3\Pi_{\pm 1u}$, and $^3\Pi_{\pm 2u}$ of the $b\,^3\Pi_u$ state are mixed due to the transition from Hund's case (a) to Hund's case (b) [20,25]. The 0_u^+ state predissociates through the 1_u character gained at short range. Interaction (II) involves the Coriolis interaction through the matrix element $H^{\rm el} = \langle ^3\Pi_{0^+u}|\frac{1}{2\mu R^2}\hat{J}^+\hat{S}^-|^3\Pi_{1u}\rangle = B_{vv'}[2J(J+1)]^{1/2}$ [24], $B_{vv'} = \langle \chi_{v,J}|\frac{\hbar^2}{2\mu R^2}|\chi_{v',J}\rangle$, near the crossing point at $R \sim 17$ Å. Interaction (III) is the well known spin-orbit interaction which mixes the triplet $b\,^3\Pi_{0^+u}$ state and the singlet $A\,^1\Sigma_u^+$ state. According to the rigorous selection rule $\Delta J = 0$, interactions (I) and (II) of the 0_u^+ state with the 1_u state ($J = 1$ is the lowest rotational level) can occur only for levels $J \geq 1$, while interaction (III) with the $A\,^1\Sigma_u^+$ state ($J = 0$ is the lowest rotational level) also allows the $J = 0$ level of the 0_u^+ state to predissociate. Since interactions (II) and (III) involve real curve crossings, we can use the Landau-Zener formula to estimate the nonadiabatic transition probabilities,

$$P_{\rm LZ} = 2e^{-A}(1 - e^{-A}). \qquad (1)$$

Here $A = 2\pi(H^{\rm el})^2/\hbar vD$, v the relative velocity of the two nuclei at the curve crossing point, and D the slope difference of the two potential curves at the crossing point [20]. Considering first interaction (III), the spin-orbit matrix element $H^{\rm el} = \langle b\,^3\Pi_{0^+u}|H^{\rm SO}|A\,^1\Sigma_u^+\rangle$ has been measured to be 18.4 cm^{-1} for K$_2$ [26]. The slope difference of the two potential curves at $R = 4.7$ Å is 1715 cm$^{-1}/$Å [27]. Vibrational levels of the 0_u^+ state between the two fine-structure asymptotes have kinetic energies ~ 6414 to 6471 cm^{-1} relative to the crossing point. The Landau-Zener probabilities for these levels are estimated to be $P_{\rm LZ} = 0.017$ to 0.016. The probability for interaction (II) is found to be even smaller $P_{\rm LZ} = 4 \times 10^{-5}$, due to the very small rotational constants ($B_v \sim 0.007$ cm^{-1}) near the crossing point.

For interaction (I), we instead use the observed line broadening to give an estimation of the near-threshold total predissociation probability of the 0_u^+ state. The last eight observed spectral lines of the 0_u^+ state near the dissociation limit in the dashed rectangle are shown in the inset of Fig. 2(c). Their FWHM widths are listed in

TABLE I. Estimated lower and upper bounds of the near-threshold total predissociation probabilities (P_{LB} and P_{UB}) of the eight vibrational levels of the 0_u^+ state. The uncertainty for ΔE_v and γ_{obs} is the uncertainty in reading the laser frequencies (30 MHz).

ΔE_v (GHz)	B_v (GHz)	γ_{obs} (GHz)	P_{LB}	P_{UB}
3.52(3)	0.0141	0.86(3)	0.16(2)	0.20(2)
3.31(3)	0.0133	0.86(3)	0.17(2)	0.22(2)
3.03(3)	0.0124	0.86(3)	0.19(2)	0.24(2)
2.73(3)	0.0117	0.83(3)	0.20(2)	0.25(2)
2.51(3)	0.0109	0.80(3)	0.21(2)	0.26(2)
2.39(3)	0.0102	0.80(3)	0.22(2)	0.27(2)
2.20(3)	0.0096	0.73(3)	0.21(2)	0.27(2)
1.96(3)	0.0089	0.61(3)	0.18(3)	0.24(3)

Table I. We estimate the line broadening due to predissociation by subtracting from the observed linewidths a Lorentzian power broadening width of 146(21) MHz inferred from the rotationally resolved 1_g state spectrum [28]. Under the ultracold condition ($T < 1$ mK), only the lowest four rotational levels $J = 0$ to $J = 3$ of the 0_u^+ state are excited. Among them, $J = 1$ should have the highest excitation intensity due to the dominant s-wave contribution [5]. Since no rotational structure is resolved for the 0_u^+ state in our fragmentation spectra, accurate rotational corrections to the observed linewidths cannot be obtained. For vibrational levels near the dissociation limit, however, the rotational spacings are small compared with the observed linewidths (B_v is <2% of the observed linewidths). We therefore can estimate an upper bound of the predissociation line broadening by assuming a single rotational line contribution and a lower bound by subtracting a maximum rotational contribution of $12B_v$ (the separation between $J = 0$ and $J = 3$) from the observed linewidths. Table I shows the vibrational spacings $\Delta E_v = (E_{v+1} - E_{v-1})/2$, the calculated rotational constants B_v, the observed linewidths γ_{obs}, and the estimated lower and upper bounds of the total predissociation probabilities, $P = \gamma_{corr}/\Delta E_v$, of the eight near-threshold vibrational levels. The estimated lower and upper bounds have average values of $P = 0.19(2)$ and $0.24(2)$, respectively. This total predissociation probability of the 0_u^+ state [for all three interactions (I)–(III)] is more than 1 order of magnitude larger than the sum for interactions (II) and (III) ($P \sim 0.016$). This means that interaction (I) is the dominant mechanism for the predissociation of the 0_u^+ state, in agreement with the theoretical prediction [20]. Our estimated near-threshold total probability, however, is about a factor of 2 larger than the calculated value of $P = 0.12$ at threshold for 0_u^+ FS-changing collisions at $T \sim 1$ mK [20]. The reason for the difference is not presently understood, but our estimation seems to confirm the existing factor of 2 discrepancy between theory and experiment [20].

In conclusion, we have observed high quality photoassociation spectra of the predissociating long-range 1_g and 0_u^+ states of $^{39}K_2$ by fragmentation spectroscopy. The near-threshold predissociation analysis shows that the 0_u^+ state is an important channel for FS-changing collisions while the contribution from the 1_g interaction is negligible. The use of fragmentation spectroscopy in ultracold photoassociation experiment may prove even more powerful for heavier species, e.g., Rb and Cs since they will have higher predissociation rates due to their stronger spin-orbit interactions.

[1] H. R. Thorsheim, J. Weiner, and P. S. Julienne, Phys. Rev. Lett. **58**, 2420 (1987).
[2] P. D. Lett, P. S. Julienne, and W. D. Phillips, Annu. Rev. Phys. Chem. **46**, 423 (1995).
[3] K. M. Jones et al., Europhys. Lett. **35**, 85 (1996).
[4] H. Wang, P. L. Gould, and W. C. Stwalley, J. Chem. Phys. **106**, 7899 (1997).
[5] K. M. Jones et al., Phys. Rev. A **54**, R1006 (1996).
[6] W. I. McAlexander, E. R. I. Abraham, and R. G. Hulet, Phys. Rev. A **54**, R5 (1996).
[7] H. Wang et al., Phys. Rev. A **55**, R1569 (1997).
[8] E. R. I. Abraham et al., Phys. Rev. Lett. **74**, 1315 (1995).
[9] J. R. Gardner et al., Phys. Rev. Lett. **74**, 3764 (1995).
[10] E. Tiesinga et al., J. Res. Natl. Inst. Stand. Technol. **101**, 505 (1996).
[11] C. C. Tsai et al., Phys. Rev. Lett. **79**, 1245 (1997).
[12] K. M. Jones et al., J. Phys. B **30**, 289 (1997).
[13] H. Wang et al., Phys. Rev. Lett. **78**, 4173 (1997).
[14] D. Leonhardt and J. Weiner, Phys. Rev. A **52**, R4332 (1995).
[15] W. C. Stwalley, Y.-H. Uang, and G. Pichler, Phys. Rev. Lett. **41**, 1164 (1978).
[16] X. T. Wang, H. Wang, P. L. Gould, W. C. Stwalley, E. Tiesinga, and P. S. Julienne (to be published).
[17] R. A. Cline, J. D. Miller, and D. J. Heinzen, Phys. Rev. Lett. **73**, 632 (1994).
[18] P. A. Molenaar, P. van der Straten, and H. G. M. Heideman, Phys. Rev. Lett. **77**, 1460 (1996).
[19] A. Gallagher and D. E. Pritchard, Phys. Rev. Lett. **63**, 957 (1989).
[20] P. S. Julienne and J. Vigue, Phys. Rev. A **44**, 4464 (1991).
[21] A. Fioretti et al., Phys. Rev. A **55**, R3999 (1997).
[22] D. Hoffmann, P. Feng, and T. Walker, J. Opt. Soc. Am. B **11**, 712 (1994).
[23] No reproducible signals above noise level at the position of $v = 90$ were recorded.
[24] H. Lefebvre-Brion and R. W. Field, *Perturbations in The Spectra of Diatomic Molecules* (Academic Press, Inc., New York, 1986), p. 37.
[25] J. B. Atkinson, J. Becker, and W. Demtroder, Chem. Phys. Lett. **87**, 92 (1982).
[26] A. J. Ross et al., J. Phys. B **20**, 6225 (1987).
[27] G. Jong et al., J. Mol. Spectrosc. **155**, 115 (1992).
[28] Multiplying the power broadening of 140(20) MHz for the 1_g state by $(A_{0u^+}/A_{1g})^{1/2} = (1.3A_{4p}/1.2A_{4p})^{1/2} = 1.04$, where A_x is the spontaneous decay rate.